Simulation of Ca-Calmodulin-Dependent Protein Kinase II on Rabbit Ventricular Myocyte Ion Currents and Action Potentials

Eleonora Grandi,*† Jose L. Puglisi,† Stefan Wagner,‡ Lars S. Maier,‡ Stefano Severi,* and Donald M. Bers†
*Biomedical Engineering Laboratory, Department of Electronics, Computer Science and Systems, University of Bologna, Bologna, Italy; †Department of Physiology, Loyola University, Chicago, Illinois; and ‡Department of Cardiology and Pneumology, Georg-August-University, Göttingen, Germany

ABSTRACT Ca-calmodulin-dependent protein kinase II (CaMKII) was recently shown to alter Na^+ channel gating and recapitulate a human Na^+ channel genetic mutation that causes an unusual combined arrhythmogenic phenotype in patients: simultaneous long QT syndrome and Brugada syndrome. CaMKII is upregulated in heart failure where arrhythmias are common, and CaMKII inhibition can reduce arrhythmias. Thus, CaMKII-dependent channel modulation may contribute to acquired arrhythmic disease. We developed a Markovian Na^+ channel model including CaMKII-dependent changes, and incorporated it into a comprehensive myocyte action potential (AP) model with Na^+ and Ca^{2+} transport. CaMKII shifts Na^+ current (I_{Na}) availability to more negative voltage, enhances intermediate inactivation, and slows recovery from inactivation (all loss-of-function effects), but also enhances late noninactivating I_{Na} (gain of function). At slow heart rates, with long diastolic time for I_{Na} recovery, late I_{Na} is the predominant effect, leading to AP prolongation (long QT syndrome). At fast heart rates, where recovery time is limited and APs are shorter, there is little effect on AP duration, but reduced availability decreases I_{Na}, AP upstroke velocity, and conduction (Brugada syndrome). CaMKII also increases cardiac Ca^{2+} and K^+ currents (I_{Ca} and I_{to}), complicating CaMKII-dependent AP changes. Incorporating I_{Ca} and I_{to} effects individually prolongs and shortens AP duration. Combining I_{Na}, I_{Ca}, and I_{to} effects results in shortening of AP duration with CaMKII. With transmural heterogeneity of I_{to} and I_{to} downregulation in heart failure, CaMKII may accentuate dispersion of repolarization. This provides a useful initial framework to consider pathways by which CaMKII may contribute to arrhythmogenesis.

INTRODUCTION

Cardiac sodium (Na^+) channels control cardiac excitability and the velocity of impulse propagation by initiating the action potential (AP). Different disorders in heart excitability have been related to derangement of the cardiac Na^+ channel (1). A number of inherited diseases associated with mutations in SCN5A, the gene encoding the α-subunit of the cardiac Na^+ channel, have been discovered and linked to long QT type 3 (LQT3) and Brugada (BrS) syndromes, conduction diseases, and structural defects. Notably, mutations showing overlapping phenotypes have been characterized. A single human mutation (1795InsD) in SCN5A is linked to simultaneous LQT3 and BrS features. This 1795InsD mutation in humans has been studied in expressed Na^+ channels (2). The mutant Na^+ current (I_{Na}) exhibits increased intermediate inactivation and slowed recovery from inactivation, and the mutant Na^+ channel availability is shifted to more negative potentials, all of which would reduce I_{Na} (loss of function) and could explain Brugada-like symptoms in patients at faster heart rates. In addition, this 1795InsD mutation causes persistent I_{Na}, which fails to completely inactivate during long-duration APs. The persistent I_{Na} would produce a gain of function, and that could contribute to AP prolongation and LQT syndrome. This would be especially pronounced at slow heart rates where I_{Na} recovery from inactivation may be more complete (even with the mutation) and where the longer intrinsic AP duration (APD) would increase the impact of the late I_{Na}.

Na^+ channel gating may also be altered in acquired diseases, e.g., drug-induced LQT syndrome, cardiac ischemia, and heart failure (HF). In HF, altered Na^+ channel regulation could cause widespread acquired Na^+ channel dysfunction and arrhythmogenesis. For example, Ca-calmodulin-dependent protein kinase II (CaMKII) is upregulated and also more active in HF (3). Wagner et al. (4) recently showed that CaMKII alters cardiac myocyte Na^+ channel gating in a manner very similar to the combined LQT/Brugada genetic phenotype mentioned above (1795InsD). Adenovirus-mediated (acute) and transgenic (chronic) overexpression of the cytosolic δ isoform (CaMKIIδc) shifted voltage dependence of Na^+ channel availability to more negative membrane potentials, enhanced intermediate inactivation, and slowed recovery from inactivation (and these effects were prevented by CaMKII inhibitors). In addition, CaMKIIδc markedly increased persistent (late) inward I_{Na} and intracellular $[Na^+]$ ($[Na^+]_i$). From these alterations, one might expect less Na^+ channel availability at fast heart rates but more inward I_{Na} during long APs at slow heart rates.

The increased levels of CaMKII in HF may target several myocyte proteins (5). CaMKII phosphorylates Ca^{2+} transport proteins such as phospholamban (6), ryanodine receptors

Submitted June 12, 2007, and accepted for publication August 1, 2007.

Address reprint requests to Donald M. Bers, PhD, Dept. of Physiology, Loyola University, Chicago, Stritch School of Medicine, 2160 South First Ave., Maywood, IL 60153. Tel.: 708-216-1018; Fax: 708-216-6308; E-mail: dbers@lumc.edu.

Editor: David A. Eisner.

0006-3495/07/12/3835/13 $2.00

doi: 10.1529/biophysj.107.114868

(7–9), and L-type Ca^{2+} channels (8,10,11). In addition, CaMKII can also modulate K^+ channels (12–15). CaMKII is known to mediate Ca^{2+}-dependent I_{Ca} facilitation (8,10,11), and Kohlhaas et al. (8) showed that CaMKII overexpression in rabbit myocytes increases peak I_{Ca} and slows inactivation (possibly related to I_{Ca} facilitation). CaMKII can also modulate transient outward K^+ current (I_{to}). Wagner et al. (15) showed that upon CaMKII overexpression, the expression levels of $K_v1.4$ channels (responsible for the slow component of I_{to}) are enhanced, as is the current recovery from inactivation. Given the multiple CaMKII targets, it is difficult a priori to discern the relative effects of CaMKII modulation of I_{Na}, I_{Ca}, and I_{to} on ventricular myocyte APs. In this study, we simulate the CaMKII-induced alterations of I_{Na}, I_{Ca}, and I_{to} (individually and collectively) on the rabbit ventricular AP.

Mathematical models have been widely used to simulate the voltage-dependent gating of ion channels. Composite models of ion channels and excitation-contraction coupling (ECC) allow investigation of the effects of altered Na^+ channel kinetic properties on myocyte electrical activity (16–18). Clancy and Rudy (16) showed that a theoretical AP model could simulate the 1795InsD mutant current behavior by including an extended formulation of their Markovian Na^+ channel structure that incorporates a bursting mode. Here, we used a variation of this Markovian Na^+ channel model to simulate the CaMKIIδc effects on I_{Na} reported by Wagner et al. (4) and we incorporate this into a comprehensive AP and ECC model of rabbit ventricular myocytes (19). We also incorporated CaMKII-dependent effects on I_{Ca} and I_{to} in rabbit ventricular myocytes to distinguish the independent and combined effects of these CaMKII targets on APD.

METHODS

Na^+ current model simulation

The Markov model structure (Fig. 1) implemented in this study is based on that proposed by Clancy and Rudy (16,17). It contains two modes of gating, a background mode and a burst mode. The background mode reflects the normal sequence of activation and inactivation that most channels undergo upon depolarization and contributes predominantly to the large transient component of I_{Na}. The burst mode reflects a small population of channels that transiently fail to inactivate during the AP plateau and results in a sustained inward current. The background mode includes the nine states in the upper two rows, consisting of three closed states (*C3*, *C2*, and *C1*), a conducting open state (*O*), a fast inactivation state (*IF*), and two intermediate inactivation states (*IM1* and *IM2*) that are required to reproduce the complex fast and slow recovery features of I_{Na} inactivation. The lower four states in Fig. 1 correspond to the burst or late mode (prefix *L*), in which inactivation does not occur. Voltage (V_m)-independent transition rates between upper and lower states represent a probability of transition between the two modes of gating.

Table 1 shows the expressions of the transition rates between the Markov model states. The corresponding parameters were identified by a fitting procedure to simulate the electrophysiological characterization of cardiac I_{Na} in βGal and in CaMKIIδc-overexpressing rabbit myocytes reported by Wagner et al. (4). The following voltage-clamp protocols were simulated for parameter identification: activation, steady-state inactivation, intermediate inactivation, recovery from inactivation, and long-depolarization voltage step to assess late I_{Na}. The model results for each protocol were compared with experimental data. The transition rate parameters that maximally influence each voltage-clamp protocol were identified with an automatic procedure. Namely, the ratio a_8/b_8 was modified to reproduce the experimental data accounting for late I_{Na}; a_5/b_5 was tuned to correctly simulate the channel availability curve; a_6, b_6 and a_7, b_7 were adjusted to represent the observed characteristics of intermediate inactivation and recovery from inactivation. The Nelder-Mead simplex direct algorithm was used to find the parameter values minimizing the sum of the least-square errors between model predictions and experimental data for each protocol. The values proposed by Clancy and Rudy (16) were chosen as initial guesses in the minimization procedure to identify the transition rate parameters that allowed the best fitting of our βGal data. The identified βGal set in Table 2 was subsequently used as an initial guess to identify the CaMKIIδc channel parameters. The parameters that influence more than one protocol were then manually tuned to optimize fitting to all the experimental data. A full list of the parameters is given in Table 2. Matlab 7 and Simulink (The MathWorks, Natick, MA) were used for all numerical computations.

L-type Ca^{2+} current simulation

The L-type Ca^{2+} current formulation of Shannon et al. (19) was modified to reproduce the effects of CaMKII (8) by increasing the channel maximal conductance by 10% and mimicking Ca^{2+}-dependent facilitation with an additional term that makes the Ca^{2+}-dependent inactivation less complete.

In βGal-overexpressing cardiomyocytes, Ca^{2+}-dependent inactivation (local $K_{d(Ca)} = 7\ \mu M$) is modeled by using the variable f_{Ca}, in which dynamic changes are described as

$$f_{Ca} = 1 - f_{CaB}$$

$$\frac{df_{CaB}}{dt} = 1.7[Ca^{2+}]_c(1 - f_{CaB}) - 0.0119 f_{CaB},$$

where $[Ca^{2+}]_c$ is the $[Ca^{2+}]$ in the actual compartment (either junctional or subsarcolemmal space, in mM).

To account for CaMKII overexpression, the Ca^{2+}-dependent inactivation variable becomes

$$f_{Ca} - f_{Ca,CaMKII},$$

where

$$f_{Ca,CaMKII} = \frac{0.1}{1 + \frac{0.01}{[Ca^{2+}]_c}}.$$

Transient outward K^+ current simulation

The formulations of the slow and fast component of I_{to} were adapted from Bassani et al. (20) to account for the increased expression levels of $K_v1.4$ channels and for the enhanced recovery from inactivation in CaMKII-overexpressing rabbit myocytes (15). To this purpose, maximal conductance of the slow component $G_{to,slow}$ was increased by 50% in the CaMKII model and the time constants of $I_{to,slow}$ inactivation were modified as follows:

$$\tau_{Yto,s} = \frac{P_y}{1 + e^{\frac{V + 33.5}{10}}} + 1$$

$$\tau_{Rto,s} = \frac{P_{R1}}{1 + e^{\frac{V + 33.5}{10}}} + P_{R2}.$$

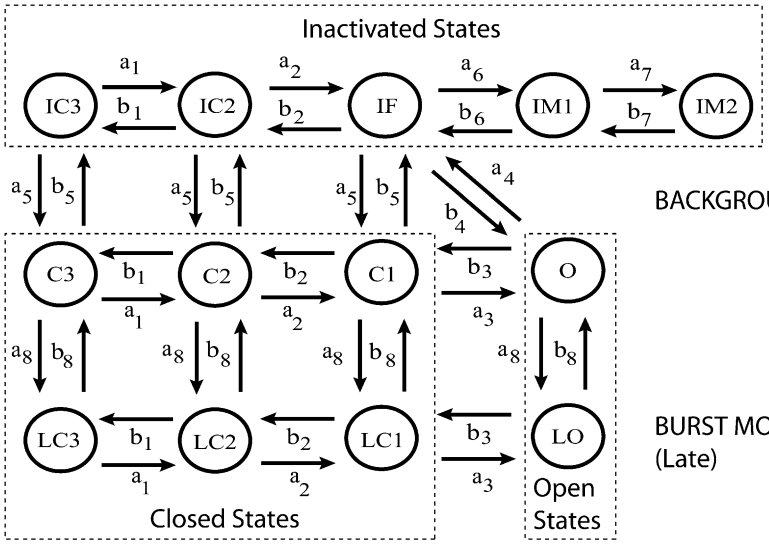

FIGURE 1 Markov model of the cardiac Na^+ channel. The channel model contains background (*upper nine states*) and burst (*lower four states*) gating modes. The burst mode reflects a population of channels that transiently fail to inactivate and accounts for a sustained inward current (or late current).

Values of P_y, P_{R1}, and P_{R2} are (in ms) 182, 8085, and 131, respectively, for βGal and 15, 3600, and 500, respectively, for CaMKII-overexpressing cardiomyocytes.

Action potential simulation

The ventricular AP was simulated using the Chicago model of rabbit ventricular myocyte (19), which includes both a cleft space (between sarcoplasmic reticulum (SR) and sarcolemmal membrane) and a separate subsarcolemmal compartment (where sarcolemmal ion channels and transporters sense higher $[Ca^{2+}]_i$ than in the bulk cytosol). The model was implemented in Matlab 7 (The MathWorks, Natick, MA). The model was adjusted to correctly describe the ratio between slow and fast components of I_{to} to reproduce the experimental APD adaptation to the pacing rate observed in rabbit myocytes (21). For this purpose, the conductances of $I_{to,fast}$ and $I_{to,slow}$ were set to 0.02 and 0.06 mS/μF, respectively.

The I_{Na} model was replaced with the above Markov model. Maximal conductance G_{Na} at 37°C was calculated as 23 mS/μF for both βGal and CaMKII ($Q_{10} = 1.5$ for Na^+ channel conductance (22)). The kinetic rates were normalized to 37°C with a Q_{10} of 2.1 (22). I_{Ca} was similarly scaled up to 37°C, using our previous measurements in rabbit ventricular myocytes at 25°C and 35°C (23). Total I_{to} density was lower in rabbit ventricular myocytes expressing βGal after 24–36 h in culture (15), compared to freshly isolated myocytes (20). To better reflect the physiological situation for AP simulations, we used fresh myocyte I_{to} amplitudes ($I_{to,fast}$ and $I_{to,slow}$) for control and relative changes caused by CaMKII versus βGal overexpression to simulate the CaMKII case. Pacing was simulated by a current pulse train (pulses of 5 ms in duration) of 9.5 A/F in amplitude with different frequencies (0.1, 0.25, 0.5, 1, 2, and 3 Hz). A variable order solver based on the numerical differentiation formulas was used to numerically solve the model equations (ode15s) (24). The stimulation was maintained until a steady AP was reached (typically ~100 s).

TABLE 1 Transition rate expressions (ms^{-1})

Transition rates
$a_1 = (P_{1a1}/(P_{2a1}\exp(-V_m/17) + 0.20\exp(-V_m/150)))$
$a_2 = (P_{1a1}/(P_{2a1}\exp(-V_m/15) + 0.23\exp(-V_m/150)))$
$a_3 = (P_{1a1}/(P_{2a1}\exp(-V_m/12) + 0.25\exp(-V_m/150)))$
$b_1 = P_{1b1}\exp(-V_m/P_{2b1})$
$b_2 = P_{1b2}\exp(-(V_m - P_{2b2})/(P_{2b1}))$
$b_3 = (P_{1b3}\exp(-(V_m - P_{2b3})/(P_{2b1})))$
$a_5 = P_{1a5}\exp(-V_m/P_{2a5})$
$b_5 = (P_{1b5} + P_{2b5}\,V_m)$
$a_4 = (P_{1a4}\exp(V_m/P_{2a4}))$
$b_4 = (a_3\,a_4\,a_5)/(b_3\,b_5)$
$a_6 = a_4/P_{1a6}$
$b_6 = P_{1b6}\exp(-V_m/P_{2b6})$
$a_7 = (P_{1a7}\exp(V_m/P_{2a7}))$
$b_7 = P_{1b7}\exp(-V_m/P_{2b7})$
$a_8 = P_{1a8}$
$b_8 = P_{1b8}$

TABLE 2 Na^+ channel model parameters for βGal and CaMKII channels

Parameters	βGal	CaMKII
P_{1a1}	3.802	
P_{2a1}	0.1027	
P_{1a4}	9.178	
P_{2a4}	25	
P_{1a5}	$3.7933e^{-7}$	
P_{2a5}	7.7	
P_{1b1}	0.1917	
P_{2b1}	20.3	
P_{1b2}	0.2	
P_{2b2}	5	
P_{1b3}	0.22	
P_{2b3}	10	
P_{1b5}	0.0042	0.0067
P_{2b5}	$2e^{-6}$	
P_{1a6}	100	
P_{1b6}	$8.8061e^{-7}$	$7.0449e^{-7}$
P_{2b6}	11.3944	
P_{1a7}	$0.3543e^{-3}$	$0.6377e^{-3}$
P_{2a7}	23.2696	
P_{1b7}	$0.2868e^{-3}$	
P_{2b7}	35.9898	
P_{1a8}	$4.7e^{-7}$	$11.75e^{-7}$
P_{1b8}	$9.5e^{-4}$	

RESULTS

Na^+ current simulation

Steady-state inactivation and activation

Fig. 2 shows experimental data (7) and simulations, which confirm the adequacy of the Na^+ channel Markovian model. Table 3 shows sources of experimental data used for validation of the simulations here. To assess the voltage dependence of steady-state inactivation (or availability), I_{Na} was measured during test pulses to −20 mV (20 ms) after 500-ms prepulses from −140 mV to various V_m (with 10-mV increments). As in the experimental data, CaMKIIδc overexpression shifts inactivation to more negative potentials with respect to βGal (Fig. 2 *A*).

Steady-state activation was not altered by CaMKIIδc in the experimental data (4). This was assessed by 40-ms depolarizations from a holding potential of −140 mV to −80/+60 mV (with 10-mV increments). Relative conductance was taken by dividing peak I_{Na} by the driving force ($V_m - E_{Na}$). The resulting conductance was normalized to the maximal chord conductance. As in the experimental data, simulated CaMKIIδc overexpression does not affect I_{Na} activation with respect to βGal (Fig. 2 *B*; note that βGal and CaMKIIδc traces are superimposed).

Recovery from inactivation and intermediate inactivation

Recovery from inactivation was investigated using a 1000-ms depolarization to –20 mV, which initiates fast and intermediate inactivation (P_1), followed by a recovery interval of variable duration and a subsequent test pulse (P_2). CaMKIIδc slows recovery from inactivation in our simulations, as well as in the experimental results (Fig. 2 *C*). Accumulation of intermediate inactivation was assessed using depolarizations of variable duration (P_1) followed by a 20-ms recovery period at −140 mV (which allows channel recovery from fast inactivation). Na^+ channels that have undergone intermediate inactivation would still be largely unavailable, causing a reduction in I_{Na} at the subsequent test pulse P_2 to −20 mV. In the computer simulations, as in the experimental recordings, intermediate inactivation is enhanced by CaMKIIδc (Fig. 2 *D*).

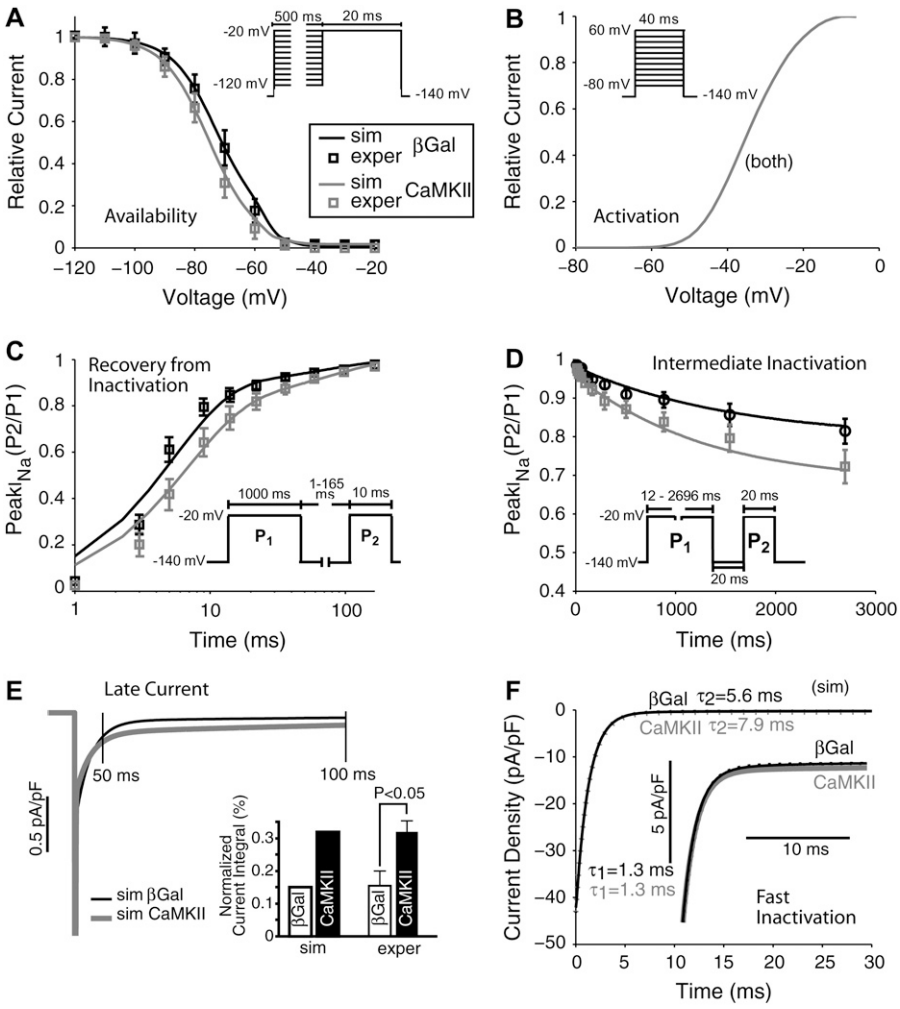

FIGURE 2 Experimental (*squares*) and simulated (*solid lines*) voltage-clamp protocols for βGal- (*black*) and CaMKII-modulated (*gray*) Na^+ channels (data at 140 mM external Na^+ concentration). (*A*) Steady-state inactivation. CaMKIIδc overexpression shifts the availability curve toward negative potentials. (*B*) Activation. Na^+ channel activation is not affected by CaMKIIδc overexpression (traces are superimposed). (*C* and *D*) CaMKIIδc slows the recovery from inactivation (*C*) and enhances the intermediate inactivation (*D*). (*E*) Late I_{Na} is enhanced by CaMKIIδc overexpression. Simulated traces are shown at left, and bar graphs of simulated and experimental normalized current integrals at right. (*F*) Fast and slow time constants of I_{Na} decay. Acute CaMKIIδc overexpression slows the late component of fast I_{Na} inactivation. Experimental data are from Wagner et al. (15).

TABLE 3 CaMKII overexpression data

Figure	Measure	Source	Experiment
Fig. 2	I_{Na}	Wagner et al. (4)	Rabbit myocyte, 22°C, ruptured patch clamp
Fig. 4	$[Na^+]_i$	Wagner et al. (4)	Rabbit myocyte, 22°C, ruptured patch clamp
Fig. 5	I_{Ca}	Kohlhaas et al. (8)	Rabbit myocyte, 22°C, ruptured patch clamp
Fig. 6	I_{to}	Wagner et al. (15)	Rabbit myocyte, 22°C, ruptured patch clamp
Fig. 8	AP	Wagner et al. (15)	Rabbit myocyte, 22°C, ruptured patch clamp

Late current

CaMKIIδc enhances late I_{Na}. Currents were elicited by 1000-ms depolarizations to −20 mV (from −140 mV), and normalized to peak I_{Na}. The current integral was calculated between 50 and 500 ms (Fig. 2 *E*) and plotted relative to the I_{Na} integral if no inactivation had occurred (i.e., peak current × 450 ms). As shown in Fig. 2 *E*, compared to control, simulated CaMKIIδc overexpression resulted in a larger late I_{Na}. These results fit the experimental data (4) shown for comparison in Fig. 2 *E*.

Fast inactivation

CaMKIIδc slows fast Na^+ channel inactivation in rabbit CaMKIIδc myocytes compared to βGal (Fig. 2 *F*). The Na^+ current decay (first 50 ms) was fitted with a double exponential function. Fits (*dotted lines*) to the simulated traces (*solid lines*) and corresponding parameters τ_1 and τ_2 (ms) are shown in black (βGal) and gray (CaMKIIδc). The deceleration of current decay was most prominent in the late component (at right in Fig. 2 *F*), so that τ_2 was greater compared to control (7.8 vs. 5.6 ms), whereas τ_1 appeared to be unchanged (1.3 ms), in agreement with Wagner et al. (4).

CaMKII-dependent Na^+ current alterations on AP and $[Na^+]_i$

The simulations of the effect of the CaMKII-dependent Na^+ channel kinetic alterations on ventricular AP are shown in Fig. 3 for three pacing rates (3, 1, and 0.25 Hz). Na^+ channel modulation did not change overall AP morphology with respect to βGal. The βGal AP (*black line*) exhibits a characteristic AP shape and its duration (185, 288, and 354 ms) shows the typical rabbit APD dependence on pacing frequency (Fig. 3 *E*, *black symbols*). CaMKII APs (*gray line*) exhibit distinctive rate-dependent durations (Fig. 3 *E*, *gray symbols*). At fast rates (3 Hz), the CaMKII AP is grossly superimposable on the control AP (Fig. 3 *A*, $APD_{90} = 188$ ms). However, the short recovery interval limits Na^+ channel recovery in the CaMKII case, resulting in reduced I_{Na} amplitude, slight decrease in AP peak, and reduced AP upstroke velocity (maximum dV_m/dt; see Fig. 3 *A*, *inset*). At low frequencies, AP upstroke velocity is reduced by ~10% by the CaMKII effect, but this decrease becomes more prominent at higher frequencies (Fig. 3 *D*). This Na^+ channel loss of function would reduce AP rate of rise and conduction velocity, especially at fast heart rates. At lower rates (Fig. 3, *B* and *C*), APD is significantly prolonged,

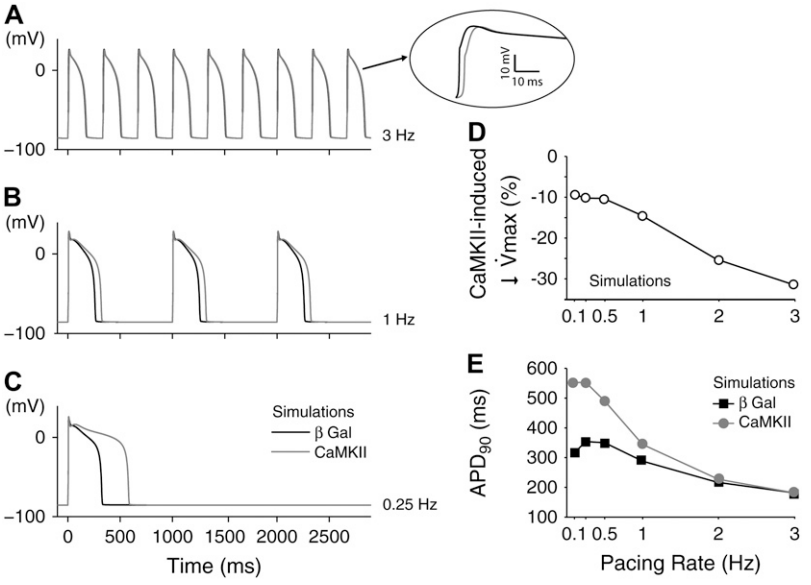

FIGURE 3 CaMKII effects on Na^+ channel gating affect the AP in a rate-dependent manner. (*A–C*) Simulations show that at slower heart rates the enhanced late I_{Na} prolongs the AP (*B* and *C*); this effect is completely blunted at faster rates (*A*), where the reduced channel availability slows down the AP upstroke (*A*, *inset*). (*D*) The upstroke velocity (dV_m/dt) is reduced upon CaMKII overexpression in a rate-dependent fashion: the faster the pacing rate, the more significant the decrease in maximum dV_m/dt. (*E*) Quantitative summary of the APD_{90} dependence on the pacing rate.

especially at the slowest rates ($APD_{90} = 344$ ms at 1 Hz and $APD_{90} = 553$ ms at 0.25 Hz). At these low frequencies, CaMKII-dependent impaired fast inactivation and enhanced late I_{Na} outweigh the slowed recovery from inactivation (because the long diastolic interval allows more complete Na^+ channel recovery). Thus, CaMKIIδc-induced AP prolongation is especially apparent at slow heart rates, and is due to the presence of a larger inward late I_{Na} during phases 2 and 3 of the AP.

Intracellular $[Na^+]$ is slightly increased at low pacing frequencies in CaMKII simulations as a result of the enhanced late I_{Na} during the AP plateau (Fig. 4 *right*). However, at faster rates, where APD is short and late I_{Na} is very small, $[Na^+]_i$ does not change significantly between βGal and CaMKII. The experimental findings of Wagner et al. (4), on the other hand, show a markedly higher $[Na^+]_i$ in CaMKII-overexpressing cardiac myocytes at all frequencies (Fig. 4 *left*). However, if we normalize the measured $[Na^+]_i$ to the value at 2 Hz (Fig. 4 *left*, *dotted line*), we again see that the increase in $[Na^+]_i$ is larger at lower frequency. The higher overall $[Na^+]_i$ seen in the experimental data suggests that our simulation fails to account for an overall gain in $[Na^+]_i$ in the myocytes with more active CaMKII. Possibly, CaMKII modulates background Na^+ influx or efflux by another mechanism.

Ca^{2+} current simulation

In both acute and chronic CaMKIIδc overexpression, L-type Ca^{2+} current was significantly increased in amplitude and exhibited some slowing of inactivation (7,8). Data from rabbit myocytes acutely overexpressing CaMKIIδc versus LacZ rabbit myocytes are shown in Fig. 5, *A* and *B*. The simulated I_{Ca} under voltage clamp produces an increase in I_{Ca} amplitude, slowing of inactivation, and unaltered voltage dependence (Fig. 5, *C* and *D*) similar to the experimental data. The larger I_{Ca} amplitude and slower inactivation would be expected to increase APD.

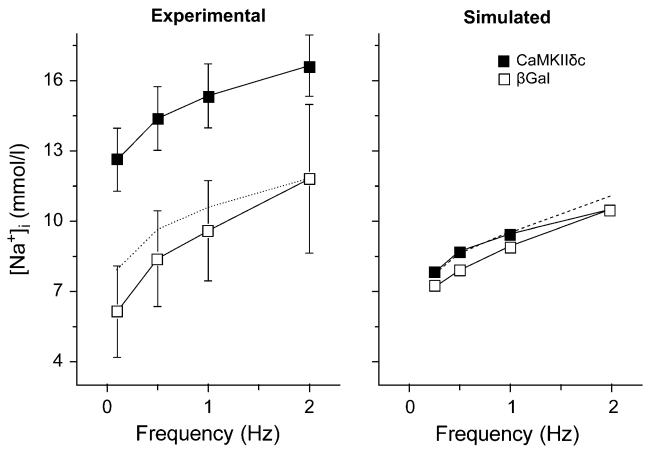

FIGURE 4 Experimental (*left*) and simulated (*right*) CaMKII effects on $[Na^+]_i$ induced by I_{Na} alterations. (*Left*) The dotted line shows the shifted experimental CaMKII data to equalize $[Na^+]_i$ at 2 Hz. (*Right*) The dashed line represents the $[Na^+]_i$ at different frequencies when I_{Na}, I_{Ca}, and I_{to} alterations due to CaMKII are incorporated into the model.

K^+ current simulation

Acute CaMKIIδc overexpression in rabbit ventricular myocytes increases I_{to} amplitude and speeds recovery from inactivation, and these effects are primarily attributable to alterations in the slowly recovering fraction of I_{to} ($I_{to,slow}$ versus $I_{to,fast}$ (15)). Fig. 6 shows the agreement between experimental and simulated effects of CaMKIIδc overexpression on I_{to}. Representative traces are shown for comparison between the recordings and the simulated currents upon voltage-clamp stimulation (Fig. 6 *G*). The V_m dependence of I_{to} (Fig. 6, *left* and *middle columns*) shows an increase in total I_{to} in both the experiments (Fig. 6 *A*) and simulations (Fig. 6 *D*). $I_{to,slow}$ amplitude was also larger in both experiments and simulations (Fig. 6, *B* and *E*), whereas no significant differences between experiments and simulations are evident for $I_{to,fast}$ (Fig. 6, *C* and *F*). $I_{to,total}$ recovery from inactivation was faster in CaMKIIδc-overexpressing rabbit myocytes (Fig. 6 *H*, *symbols*) as well as in silico (Fig. 6 *H*, *lines*). The combined CaMKII-dependent increase of I_{to} amplitude and faster $I_{to,slow}$ recovery would tend to shorten APD with CaMKII activation (i.e., opposite to that caused by the I_{Na} and I_{Ca} effects discussed above).

Impact of Na^+, Ca^{2+}, and K^+ current alterations on AP and $[Na^+]_i$

In simulations (compared with experiments), it is possible to test the impact of each individual CaMKIIδc current effect on the rabbit ventricular AP, individually or collectively. Fig. 7 *A* shows the control (βGal) AP morphology and duration (*black solid line*) at 1 Hz and Fig. 7 *B* shows APD dependence on pacing rate (Fig. 7 *B*, *black circles*). As in Fig. 3, the effects of CaMKII on I_{Na} alone tend to prolong the AP (Fig. 7 *A*, *dashed line*) especially at slow heart rates, but less so at 2 Hz pacing (Fig. 7 *B*, *diamonds*). The CaMKII-induced gain of function of I_{Ca} also prolongs APD at 1 Hz (Fig. 7 *A*, *dotted line*) and other frequencies, though less so than the I_{Na} change (Fig. 7 *B*). CaMKII-dependent I_{to} modulation alone markedly shortens the AP, and flattens the frequency dependence of APD (Fig. 7 *A* and *B*, *dash-dotted curve*).

When all three CaMKII target channels are considered (I_{Na}, I_{Ca}, and I_{to}), the net effect is that APD is reduced compared to βGal (Fig. 7, *A* and *B*, *gray line and solid circles*). The large effect of I_{to} enhancement to shorten APD appears to be dominant over the smaller effects on I_{Na} and I_{Ca} which prolong APD. However, the individual ion channel effects on APD modulation seem roughly additive. Fig. 8 shows experimental APD results in rabbit ventricular

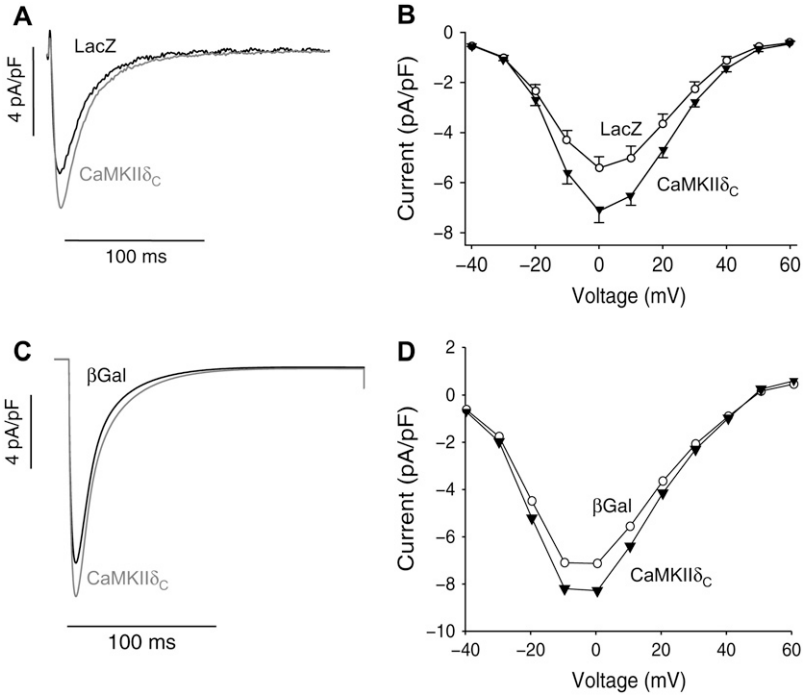

FIGURE 5 CaMKII effects on I_{Ca}. (*Left*) Experimental (*A*) and simulated (*C*) traces recorded upon a depolarization pulse. (*Right*) Experimental (*B*) and simulated (*D*) I/V relations. I_{Ca} is significantly increased in CaMKIIδc compared to control (LacZ). Inactivation is slowed by CaMKIIδc. Experimental data (*upper panels*) are from Kohlhaas et al. (8).

myocytes overexpressing CaMKIIδc: at left are the results from the study of Wagner et al. (15) and at right are those from the simulations presented in this study. CaMKIIδc overexpression shortens the rabbit ventricular APD. Over the full range of experimental measurements (0.25–2 Hz), APD was reduced by 40–50 ms in the CaMKII case compared to βGal (Fig. 8, *B* and *D*). At 0.1 Hz, the model predicts APs of similar duration for βGal and CaMKII (Fig. 8 *D*). It is

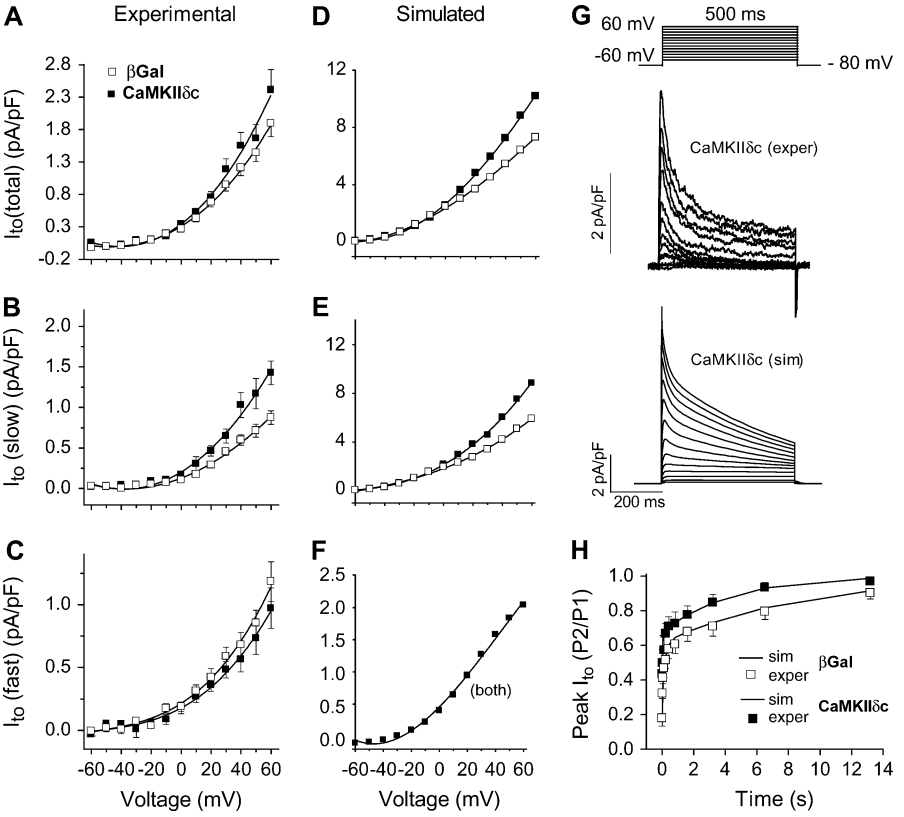

FIGURE 6 CaMKII effects on I_{to}. Experimental (*left*) and simulated (*middle*) I/V relations for total (*A* and *D*), slow (*B* and *E*), and fast (*C* and *F*) I_{to}. CaMKIIδc-mediated increase of the total current (*solid symbols*) is mainly due to CaMKIIδc effects on the slow component. (*G*) Representative current traces during voltage-clamp activation protocol for experimental (*upper*) and simulated (*lower*) CaMKII-mediated I_{to}. (*H*) Recovery from inactivation was investigated using a 500-ms depolarization pulse (from −80 mV holding potential to +50 mV) followed by recovery intervals of increasing duration and a subsequent test pulse. Recovery from inactivation was significantly increased by CaMKIIδc. Symbols represent experimental data, and lines indicate simulation results for βGal (*black*) and CaMKII (*gray*). Data are from Wagner et al. (15).

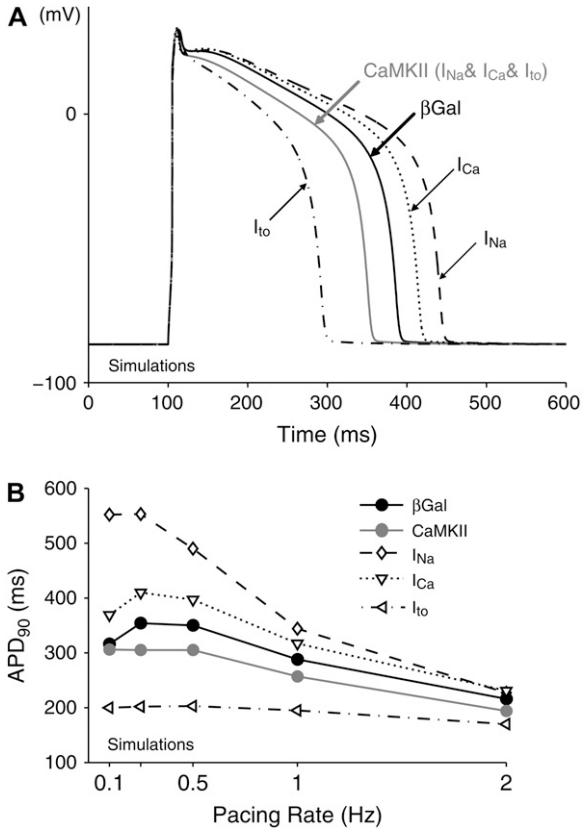

FIGURE 7 Simulated APs at 1-Hz pacing rate (*A*) and APD-frequency relations (*B*) in βGal and CaMKIIδc-overexpressing cardiac myocytes. The separate effects of each CaMKII-induced current alteration, as well as their combined impact, have been considered. CaMKII alteration of I_{Na} prolongs the AP at slow heart rate, with no effects at a 2-Hz pacing. The APD is reduced by I_{to} and increased by I_{Ca} at all frequencies. The predicted overall effect of CaMKII is AP shortening.

possible that at extremely low frequencies the more prominent late I_{Na} counteracts the enhancement of I_{to} with almost no changes in the APD.

$[Na^+]_i$ was also assessed during AP simulations. When I_{Ca} and I_{to} effects were added to the I_{Na} effect, there was slightly more CaMKII-induced rise in $[Na^+]_i$ at higher frequency (Fig. 4, *right*, *dashed line*). This might be due to higher Na^+ influx via Na^+/Ca^{2+} exchange in this situation. However, the rise in $[Na^+]_i$ still does not reach the CaMKII-dependent $[Na^+]_i$ rise seen in the experimental data (Fig. 4, *left*).

APD sensitivity to the late Na^+ current

We investigated the impact of different amounts of late I_{Na} on the APD. To this purpose, the value of the transition rate between background and bursting modes of I_{Na} (a_8) was varied. For βGal, a range of late I_{Na} integrals (normalized to peak I_{Na} if no inactivation had occurred) from 0.02 to 0.2% was explored. Accordingly, late currents ranging from 0.17% to 0.35% were reproduced for CaMKIIδc (to keep the 0.15% differential amount of late current according to experimental data). The results of this sensitivity analysis (Fig. 9) show that the noninactivating Na^+ current has a significant effect on the AP, and this effect is more pronounced at slower pacing rates (compare 0.5 and 1 Hz). Moreover, such analysis qualitatively confirms our results, since in the entire range explored, CaMKII shortens the AP with respect to βGal, independent of the actual amount of sustained I_{Na}.

APD changes with different I_{to} levels

Differences in the expression pattern of the channels responsible for $I_{to,fast}$ and $I_{to,slow}$ in different regions of the heart produce marked differences in current density and contribute to regional variations in AP duration (25). In addition, downregulation of I_{to} is a central and consistent electrophysiological change in cardiac diseases (e.g., HF) (26). Thus, different levels of I_{to} density (both fast and slow) were simulated (Fig. 10). The simulation of CaMKII has different impacts depending on I_{to} density. That is, when I_{to} is fully expressed (I_{to} 100% (Fig. 8 *C* and Fig. 10, *A* and *D*)), CaMKII shortens the AP, whereas in cells expressing 75% or 90% I_{to} reduction, the effect of CaMKII-induced I_{to} enhancement is limited (Fig. 10, *B* and *C*). In conditions where I_{to} expression is $<60\%$ (Fig. 10 *D*), net AP prolongation occurs due to the I_{Na} and I_{Ca} effects (which then outweigh the I_{to} effect).

DISCUSSION

In this study, we used an in silico approach to investigate CaMKIIδc effects on cardiac myocyte ionic currents and APs in a comprehensive computer model of ECC (19). A motivating factor was our recent report (4) that CaMKII associates with and phosphorylates the cardiac Na^+ channel and produces I_{Na} gating changes that strikingly resemble those in a human genetic mutation in Nav1.5 (1795InsD) that is linked with simultaneous arrhythmogenic LQT3 and Brugada syndrome (2). In addition, CaMKII expression is upregulated and more active in HF (3,27,28) and arrhythmias are a major cause of death in HF. There are also reports of enhanced late I_{Na} in HF (29). Thus, increased CaMKII-dependent I_{Na} modulation in HF may be an acquired arrhythmogenic Na^+ channel defect that could affect millions of people with HF (as compared with the relatively small number of individuals affected by the mechanistically informative genetic Na^+ channel mutations). Along these lines, overexpression of CaMKIIδc in transgenic mice leads to a lethal phenotype characterized by HF (30) and increased propensity to ventricular arrhythmias (4). Transgenic or pharmacologic CaMKII inhibition has also been shown to be protective against maladaptive remodeling from chronic β-adrenergic receptor stimulation, myocardial infarction (31), and arrhythmias (32). Thus, CaMKII may be a viable

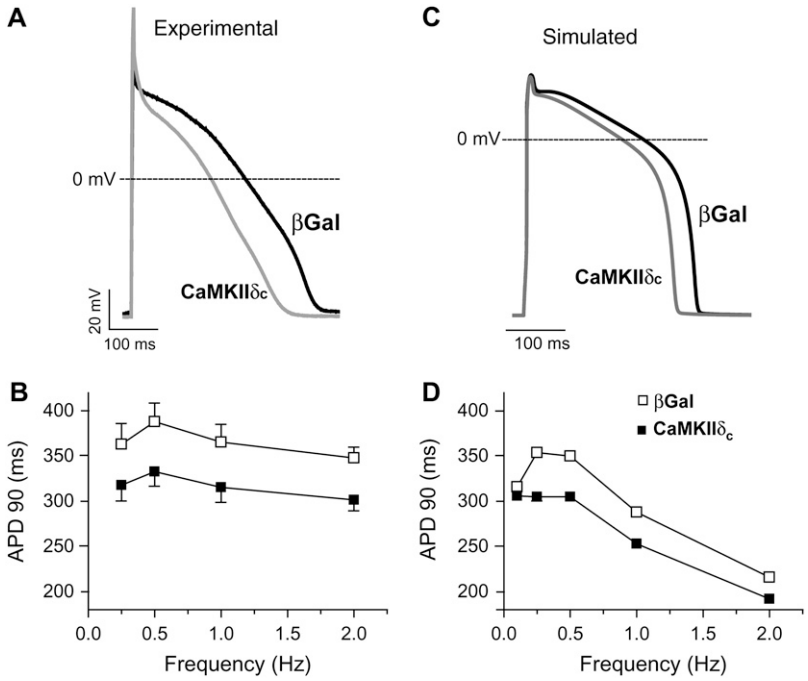

FIGURE 8 Experimental (*A* and *B*) and simulated (*C* and *D*) APs and APD-frequency relations in βGal and CaMKIIδc-overexpressing cardiac myocytes. Experimental data are from Wagner et al. (15). CaMKII shortens the AP in the entire range of pacing rates. At 0.1 Hz, where no experimental data are available, the difference between βGal and CaMKIIδc APs is negligible.

therapeutic target in the treatment of common forms of cardiac disease, and understanding how CaMKII alters ionic currents and APs is important to better understand arrhythmias that occur in conditions of CaMKII upregulation.

We focused initially on CaMKII-dependent modulation of I_{Na} (4), but we have extended the rabbit ventricular myocyte model to incorporate other channels modulated by CaMKII in heart, I_{Ca} (8) and I_{to} (15). This sort of computational approach has proven valuable to integrate information obtained at the molecular level to the whole cell and to the clinical phenotype in a number of inherited (16–18,33) and acquired (34–36) cardiac diseases.

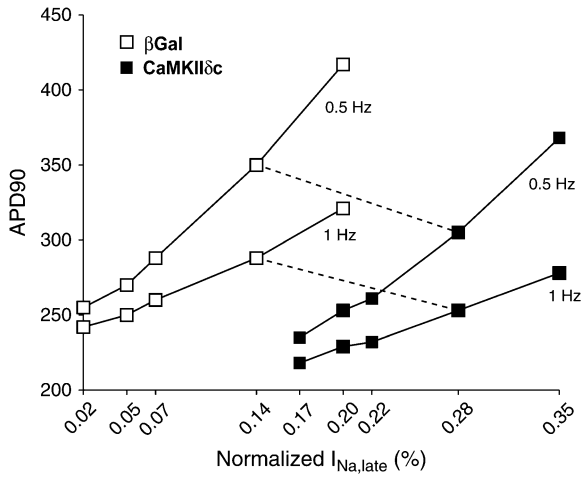

FIGURE 9 APD_{90} sensitivity to the late Na^+ current amplitude. APs were simulated by varying the amount of late Na^+ current in a range between 0.02% and 0.2% of the peak current in βGal (*open symbols*) and between 0.17% and 0.35% in CaMKII (*solid symbols*), thus keeping constant the differential current amplitude. APD changes significantly with the late current amplitude, and the sensitivity increases with the lowering of the pacing frequency (compare 0.5 and 1 Hz). Note that the results of AP shortening upon CaMKII overexpression are confirmed for any value of late Na^+ current amplitudes in the explored range.

Na^+ channel model

A Markov model of I_{Na} was identified to simulate I_{Na} measured using whole-cell patch clamp in βGal versus CaMKIIδc-overexpressing rabbit cardiomyocytes (4). This model structure has been used successfully to simulate several I_{Na} features (16–18,33). Clancy and Rudy (16) used a nine-state model (only the background mode) for the wild-type Na^+ channel. To account for long-lasting bursts experimentally observed in mutant Na^+ channels they introduced an additional mode of gating (burst mode) with a second (long-lasting and noninactivating) open state (17). Thus, the burst layer, thought to be responsible for a whole-cell persistent current, was incorporated into both our βGal and CaMKIIδc Na^+ channel models. The resulting model satisfactorily reproduces the characteristics of CaMKIIδc-modulated I_{Na} in rabbit ventricular myocytes (4) and seems suitable to analyze the effects of CaMKIIδc at the AP level.

Impact of Na^+ current alterations on AP and $[Na^+]_i$

CaMKIIδc enhances intermediate inactivation and reduces availability, at the same time impairing fast inactivation and

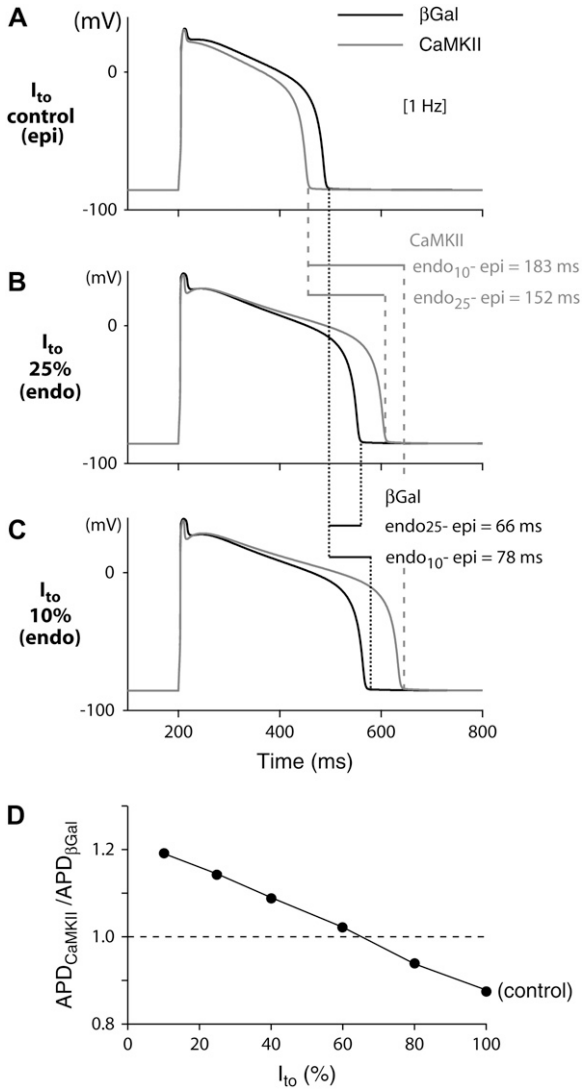

FIGURE 10 Simulated APs at 1 Hz in βGal and CaMKIIδc-overexpressing cardiac myocytes in the presence of (*A*) 100%, (*B*) 25%, and (*C*) 10% I_{to}. (*D*) Ratio of CaMKII to βGal APDs for different levels of I_{to}. When I_{to} is fully expressed (*A*, *epi*), CaMKII shortens the AP, whereas the AP is prolonged due to I_{to} downregulation (current expression <60% (*D*), e.g., *endo* (*B* and *C*)). This could amplify transmural dispersion of repolarization (endo-epi: 66 and 78 ms for βGal versus 152 and 183 ms for CaMKII), which may predispose cells to reentry phenomena.

enhancing persistent I_{Na}. These divergent alterations of I_{Na} function cause a paradoxical phenotypic overlap of LQT3 (where I_{Na} inactivation is slowed or incomplete) and Brugada syndrome (where available I_{Na} is reduced), both thought to underlie arrhythmias. Indeed, the altered Na^+ channel phenotype caused by CaMKIIδc is very similar both qualitatively and quantitatively to that caused by 1795InsD mutation in human Nav1.5, which is linked with simultaneous LQT3 and Brugada syndrome features (2).

At faster heart rates, CaMKII causes Na^+ channel accumulation in intermediate inactivation, with slow recovery therefrom, and reduces steady-state availability. The result is a loss of I_{Na} function, reduced rate of AP rise, and, consequently, slowed propagation velocity, consistent with a BrS phenotype at fast heart rate. At slow heart rates where the diastolic interval is longer, there is little loss of Na^+ channel availability (longer recovery time), and the intrinsically longer APD is further prolonged by sustained or late I_{Na}. This results in accentuated APD prolongation at slow heart rates (Fig. 3, *B*, *C*, and *E*) and an LQT3 phenotype.

It is possible that increased CaMKIIδc activity in HF may alter Na^+ channel gating, contributing to arrhythmogenesis. Indeed, noninactivating late I_{Na} is increased in human HF and failing canine hearts (29), and this could contribute to the prolonged APD characteristic of HF.

A higher sustained I_{Na} in HF due to CaMKIIδc could contribute to the elevated $[Na^+]_i$ observed in HF (37). However, the simulations here show that the I_{Na} gating changes that prolong APD are insufficient to explain the elevated $[Na^+]_i$ in either HF or CaMKII-overexpressing rabbit myocytes. Despa et al. (38) found that the elevated $[Na^+]_i$ in HF was due to increased tetrodotoxin-sensitive diastolic influx. The fact that CaMKII overexpression produced a $[Na^+]_i$ increase (4) similar to that seen in HF (38), where CaMKII is upregulated (3), suggests an untested hypothesis that CaMKII might enhance diastolic tetrodotoxin-sensitive Na^+ influx in both situations.

The slight additional rise in $[Na^+]_i$ at higher frequency when I_{Ca} and I_{to} effects of CaMKII were considered (versus I_{Na} alone), could be due to the close interplay between Na^+ and Ca^{2+} regulation in myocytes. The higher I_{Ca} and SR Ca^{2+} release would increase Na^+ influx via a Na^+/Ca^{2+} exchanger (which is the largest normal pathway for Na^+ influx in myocytes).

CaMKII has multiple targets that may alter AP

Although Na^+ channel alterations can result in gain or loss of function, depending on the pacing frequency, CaMKII modulation of I_{Ca} and I_{to} produced only gain of function at all pacing rates. Enhanced I_{Ca} prolonged APD, whereas I_{to} gain of function dramatically shortened APD (Fig. 7). When considering the effects of CaMKII on I_{Na}, I_{Ca}, and I_{to} together, APD was shortened, indicating the stronger impact of the enhanced repolarizing I_{to} (compared to the combined depolarizing contributions of I_{Ca} and I_{Na}). It is noteworthy that this balance is shifted toward a net repolarizing current in a wider range of late I_{Na}, as demonstrated by the sensitivity analysis in Fig. 9.

We also included CaMKII-dependent alterations to increase the $[Ca^{2+}]_i$ affinity of the SR Ca-ATPase (simulating phospholamban phosphorylation) and sensitization of the SR Ca^{2+} release channel (not shown) using parameters similar to those used by Shannon et al. (39). Although this altered Ca^{2+} transients and APD characteristics slightly, the APD shifts reported here were not qualitatively altered. Thus,

these effects do not modify our main conclusions about I_{Na}, I_{Ca}, and I_{to} effects.

The CaMKII-induced enhancement of I_{to} would tend to prevent the LQT3 effect of late I_{Na} and I_{Ca} enhancement, and it would not ameliorate the BrS phenotype at fast heart rates. Indeed, the greater I_{to} might slightly further snub the latter part of the AP rise and the AP peak, accentuating the BrS phenotype. On the other hand, the concerted effect of CaMKII on I_{to} (with I_{Na} and I_{Ca}) may be an orchestrated response to limit APD prolongation when CaMKII is physiologically activated. In pathophysiological conditions like HF, this situation may differ. In HF there is typically a strong downregulation of I_{to} (26), and this would limit the ability of enhanced I_{to} to offset the APD prolongation resulting from I_{Na} and I_{Ca} effects (Fig. 10). The lower amplitude of SR Ca^{2+} release in HF would also limit the extent of Ca-dependent inactivation of I_{Ca}, which would also tend to prolong APD. These effects could make the HF patient (in whom APD is already long) more prone to this sort of acquired LQT3 and its arrhythmogenic consequences.

The AP-ECC model implemented here (19) is for a generic rabbit ventricular myocyte, without distinction for regional differences in channel density within the normal ventricular wall (40,41). However, in regions where I_{to} is poorly expressed (e.g., endocardium), the effects of I_{Na} and I_{Ca} might be predominant, thus potentially leading to a LQT3-like phenotype at slow heart rates (Fig. 10, *B* and *C*) and BrS phenotype at high frequencies. In regions where I_{to} is maximally expressed (e.g., epicardium), CaMKII activation or upregulation may lead to a markedly short AP, thus resembling an acquired form of short QT syndrome. In fact, although prolonged QT intervals are intuitively associated with the risk of life-threatening events, the notion of a short QT syndrome being arrhythmogenic is relatively new (42).

Heterogeneity of transmural ventricular repolarization in the heart has been linked to a variety of arrhythmic manifestations (43). If CaMKII prolongs APDs in the endocardium (Fig. 10, *B* and *C*) and shortens APDs in the epicardium (Fig. 10 *A*), this could amplify transmural dispersion of repolarization (endo-epi 66 and 78 ms for control versus 152 and 183 ms with CaMKII (Fig. 10)), thus predisposing to the development of reentrant arrhythmias. Thus, there are several potential pathways by which cardiac CaMKII activation may be arrhythmogenic, and further experimental and in silico work will be needed to clarify which pathways are most important.

Species differences and time domain of CaMKII overexpression

In striking contrast to the AP shortening shown in rabbits, we have shown that chronic CaMKII overexpression in mice significantly prolongs APD in transgenic versus wild-type mice (7,15). Mouse electrophysiology differs significantly from that of rabbit, but this difference may be simply explicable. In the mouse, with chronic overexpression of CaMKII, I_{Na} and I_{Ca} are enhanced, as in rabbit, but I_{to} is decreased. The result is that all three current changes considered here will tend to prolong APD in mouse. Thus, it is not surprising that CaMKII prolongs the APD in the transgenic CaMKIIδc mouse (and differs from rabbit). In rabbit myocytes, acute CaMKII overexpression increased I_{to} mainly by increasing I_{to} recovery from inactivation for both $I_{to,fast}$ and $I_{to,slow}$ (and this is an acute regulatory effect sensitive to CaMKII inhibitors), but there is also a minor increase in $I_{to,slow}$ functional expression. In transgenic mice chronically overexpressing CaMKIIδc, the same acceleration of I_{to} recovery from inactivation occurs (acutely blockable by CaMKII inhibition), but down-regulation of $I_{to,fast}$ (the predominant repolarizing current in mouse) and Kv4.2/3 expression causes the dominant effect to be reduced functional I_{to} (15). This raises the notion that CaMKII can have both acute regulatory effects on ion channels (via CaMKII-dependent phosphorylation), but can also alter the expression levels (via CaMKII effects to alter protein transcription, translation, or trafficking (44)). There may also be time-dependent differences in this regulation, since 24-h overexpression of CaMKII was sufficient to demonstrate upregulation of $I_{to,slow}$ (and Kv1.4), whereas the downregulation of $I_{to,fast}$ was only evident during chronic transgenic overexpression of CaMKII. Eventually, it would be valuable to incorporate these longer-term aspects of channel modulation into dynamic computational models.

CaMKII modeling in cardiac myocytes

In our model, we simply turned on the CaMKII-modified version of the modulated currents, without considering either dynamic or local changes of its activity or association with target ion channels. Recently, Hund and Rudy (45) proposed a novel theoretical model of the canine ventricular epicardial AP and Ca^{2+} cycling, including a CaMKII regulatory pathway. They investigated aspects of Ca^{2+} transient and APD rate dependence, and concluded that CaMKII is an important determinant of the rate dependence of Ca^{2+} transient but not of APD (although neither I_{Na} or I_{to} were considered as CaMKII targets). They also showed that elevated CaMKII activity increased the cell propensity to Ca^{2+} transient and APD alternans (36).

Saucerman and Bers (2007) integrated mathematical descriptions of calmodulin-dependent regulation of CaMKII and calcineurin with the Chicago ECC model in the rabbit ventricular myocyte (46). They showed how CaMKII is especially well activated in regions where local $[Ca^{2+}]_i$ is transiently high, especially in the junctional cleft near I_{Ca} and SR Ca release sites. The subsarcolemmal region, where most other ion channels (e.g., I_{Na} and I_{to}) are localized, also exhibits higher $[Ca^{2+}]_i$ than bulk cytosolic $[Ca^{2+}]_i$ (47) and would thus also be expected to exhibit more dynamic CaMKII activation.

In conclusion, we present a computational modeling approach to study how CaMKII-dependent changes in ionic currents (I_{Na}, I_{Ca}, and I_{to}) influence APD at different heart rates. This may provide novel mechanistic insights into cellular bases of acquired arrhythmogenesis in HF and other pathophysiological settings. It may also help to identify or tailor novel potential therapeutic targets.

We thank Drs. Fei Wang and Jeffrey J. Saucerman for their help in the implementation of the ECC model.

This work was supported by grants from the National Institutes of Health (HL30077 and HL80101 to D.B.) and Deutsche Forschungsgemeinschaft (MA 1982/1-5 and MA 1982/2-1 to L.S.M.).

REFERENCES

1. Tan, H. 2006. Sodium channel variants in heart disease: expanding horizons. *J. Cardiovasc. Electrophysiol.* 17(Suppl 1):S151–S157.
2. Veldkamp, M. W., P. C. Viswanathan, C. Bezzina, A. Baartscheer, A. A. M. Wilde, and J. R. Balser. 2000. Two distinct congenital arrhythmias evoked by a multidysfunctional Na^+ channel. *Circ. Res.* 86:e91–e97.
3. Ai, X., J. W. Curran, T. R. Shannon, D. M. Bers, and S. M. Pogwizd. 2005. Ca^{2+}/calmodulin-dependent protein kinase modulates cardiac ryanodine receptor phosphorylation and sarcoplasmic reticulum Ca^{2+} leak in heart failure. *Circ. Res.* 97:1314–1322.
4. Wagner, S., N. Dybkova, E. C. L. Rasenack, C. Jacobshagen, L. Fabritz, P. Kirchhof, S. K. G. Maier, T. Zhang, G. Hasenfuss, J. H. Brown, D. M. Bers, and L. S. Maier. 2006. Ca^{2+}/calmodulin-dependent protein kinase II regulates cardiac Na^+ channels. *J. Clin. Invest.* 116:3127–3138.
5. Maier, L. S., and D. M. Bers. 2007. Role of Ca^{2+}/calmodulin-dependent protein kinase (CaMK) in excitation-contraction coupling in the heart. *Cardiovasc. Res.* 73:631–640.
6. DeSantiago, J., L. S. Maier, and D. M. Bers. 2004. Phospholamban is required for CaMKII-dependent recovery of Ca transients and SR Ca reuptake during acidosis in cardiac myocytes. *J. Mol. Cell. Cardiol.* 36:67–74.
7. Maier, L. S., T. Zhang, L. Chen, J. DeSantiago, J. H. Brown, and D. M. Bers. 2003. Transgenic CaMKIIδC overexpression uniquely alters cardiac myocyte Ca^{2+} handling: reduced SR Ca^{2+} load and activated SR Ca^{2+} release. *Circ. Res.* 92:904–911.
8. Kohlhaas, M., T. Zhang, T. Seidler, D. Zibrova, N. Dybkova, A. Steen, S. Wagner, L. Chen, J. Heller Brown, D. M. Bers, and L. S. Maier. 2006. Increased sarcoplasmic reticulum calcium leak but unaltered contractility by acute CaMKII overexpression in isolated rabbit cardiac myocytes. *Circ. Res.* 98:235–244.
9. Guo, T., T. Zhang, R. Mestril, and D. M. Bers. 2006. Ca^{2+}/calmodulin-dependent protein kinase II phosphorylation of ryanodine receptor does affect calcium sparks in mouse ventricular myocytes. *Circ. Res.* 99: 398–406.
10. Yuan, W., and D. M. Bers. 1994. Ca-dependent facilitation of cardiac Ca current is due to Ca-calmodulin-dependent protein kinase. *Am. J. Physiol. Heart Circ. Physiol.* 267:H982–H993.
11. Anderson, M. E., A. P. Braun, H. Schulman, and B. A. Premack. 1994. Multifunctional Ca^{2+}/calmodulin-dependent protein kinase mediates Ca^{2+}-induced enhancement of the L-type Ca^{2+} current in rabbit ventricular myocytes. *Circ. Res.* 75:854–861.
12. Tessier, S., P. Karczewski, E.-G. Krause, Y. Pansard, C. Acar, M. Lang-Lazdunski, J.-J. Mercadier, and S. N. Hatem. 1999. Regulation of the transient outward K^+ current by Ca^{2+}/calmodulin-dependent protein kinases II in human atrial myocytes. *Circ. Res.* 85:810–819.
13. Li, J., C. Marionneau, R. Zhang, V. Shah, J. W. Hell, J. M. Nerbonne, and M. E. Anderson. 2006. Calmodulin kinase II inhibition shortens action potential duration by upregulation of K^+ currents. *Circ. Res.* 99:1092–1099.
14. Colinas, O., M. Gallego, R. Setien, J. R. Lopez-Lopez, M. T. Perez-Garcia, and O. Casis. 2006. Differential modulation of Kv4.2 and Kv4.3 channels by calmodulin-dependent protein kinase II in rat cardiac myocytes. *Am. J. Physiol. Heart Circ. Physiol.* 291:H1978–H1987.
15. Wagner, S., E. Hacker, N. Dybkova, L. Fabritz, P. Kirchhof, D. M. Bers, and L. S. Maier. 2006. Ca/calmodulin kinase II differentially modulates transient outward potassium current in heart failure. *Circulation.* 114(Suppl. II):60.
16. Clancy, C. E., and Y. Rudy. 2002. Na^+ channel mutation that causes both Brugada and long-QT syndrome phenotypes: a simulation study of mechanism. *Circulation.* 105:1208–1213.
17. Clancy, C. E., M. Tateyama, and R. S. Kass. 2002. Insights into the molecular mechanisms of bradycardia-triggered arrhythmias in long QT-3 syndrome. *J. Clin. Invest.* 110:1251–1262.
18. Vecchietti, S., E. Grandi, S. Severi, I. Rivolta, C. Napolitano, S. G. Priori, and S. Cavalcanti. 2007. In silico assessment of Y1795C and Y1795H SCN5A mutations: implication for inherited arrhythmogenic syndromes. *Am. J. Physiol. Heart Circ. Physiol.* 292:H56–H65.
19. Shannon, T. R., F. Wang, J. Puglisi, C. Weber, and D. M. Bers. 2004. A mathematical treatment of integrated Ca dynamics within the ventricular myocyte. *Biophys. J.* 87:3351–3371.
20. Bassani, R. A., J. Altamirano, J. L. Puglisi, and D. M. Bers. 2004. Action potential duration determines sarcoplasmic reticulum Ca^{2+} reloading in mammalian ventricular myocytes. *J. Physiol.* 559:593–609.
21. Pogwizd, S. M., K. Schlotthauer, L. Li, W. Yuan, and D. M. Bers. 2001. Arrhythmogenesis and contractile dysfunction in heart failure: roles of sodium-calcium exchange, inward rectifier potassium current, and residual β-adrenergic responsiveness. *Circ. Res.* 88:1159–1167.
22. Maltsev, V. A., and A. I. Undrovinas. 2006. A multi-modal composition of the late Na^+ current in human ventricular cardiomyocytes. *Cardiovasc. Res.* 69:116–127.
23. Puglisi, J. L., R. A. Bassani, J. W. Bassani, J. N. Amin, and D. M. Bers. 1996. Temperature and relative contributions of Ca transport systems in cardiac myocyte relaxation. *Am. J. Physiol. Heart Circ. Physiol.* 270:H1772–H1778.
24. Shampine, L. F., and M. W. Reichelt. 1997. The MATLAB ODE suite. *SIAM J. Sci. Comput.* 18:1–22.
25. Oudit, G. Y., Z. Kassiri, R. Sah, R. J. Ramirez, C. Zobel, and P. H. Backx. 2001. The molecular physiology of the cardiac transient outward potassium current (I_{to}) in normal and diseased myocardium. *J. Mol. Cell. Cardiol.* 33:851–872.
26. Rose, J., A. A. Armoundas, Y. Tian, D. DiSilvestre, M. Burysek, V. Halperin, B. O'Rourke, D. A. Kass, E. Marban, and G. F. Tomaselli. 2005. Molecular correlates of altered expression of potassium currents in failing rabbit myocardium. *Am. J. Physiol. Heart Circ. Physiol.* 288:H2077–H2087.
27. Kirchhefer, U., W. Schmitz, H. Scholz, and J. Neumann. 1999. Activity of cAMP-dependent protein kinase and Ca^{2+}/calmodulin-dependent protein kinase in failing and nonfailing human hearts. *Cardiovasc. Res.* 42:254–261.
28. Currie, S., C. M. Loughrey, M. A. Craig, and G. L. Smith. 2004. Calcium/calmodulin-dependent protein kinase IIδ associates with the ryanodine receptor complex and regulates channel function in rabbit heart. *Biochem. J.* 377:357–366.
29. Valdivia, C. R., W. W. Chu, J. Pu, J. D. Foell, R. A. Haworth, M. R. Wolff, T. J. Kamp, and J. C. Makielski. 2005. Increased late sodium current in myocytes from a canine heart failure model and from failing human heart. *J. Mol. Cell. Cardiol.* 38:475–483.
30. Zhang, T., L. S. Maier, N. D. Dalton, S. Miyamoto, J. Ross, Jr., D. M. Bers, and J. H. Brown. 2003. The δC isoform of CaMKII is activated in cardiac hypertrophy and induces dilated cardiomyopathy and heart failure. *Circ. Res.* 92:912–919.
31. Zhang, R., M. S. C. Khoo, Y. Wu, Y. Yang, C. E. Grueter, G. Ni, E. E. Price, W. Thiel, S. Guatimosim, L.-S. Song, E. C. Madu, A. N. Shah,

T. A. Vishnivetskaya, J. B. Atkinson, V. V. Gurevich, G. Salama, W. J. Lederer, R. J. Colbran, and M. E. Anderson. 2005. Calmodulin kinase II inhibition protects against structural heart disease. *Nat. Med.* 11:409–417.

32. Wu, Y., J. Temple, R. Zhang, I. Dzhura, W. Zhang, R. Trimble, D. M. Roden, R. Passier, E. N. Olson, R. J. Colbran, and M. E. Anderson. 2002. Calmodulin kinase II and arrhythmias in a mouse model of cardiac hypertrophy. *Circulation.* 106:1288–1293.
33. Flaim, S. N., W. R. Giles, and A. D. McCulloch. 2006. Contributions of sustained INa and IKv43 to transmural heterogeneity of early repolarization and arrhythmogenesis in canine left ventricular myocytes. *Am. J. Physiol. Heart Circ. Physiol.* 291:H2617–H2629.
34. Gima, K., and Y. Rudy. 2002. Ionic current basis of electrocardiographic waveforms: a model study. *Circ. Res.* 90:889–896.
35. Rodriguez, B., J. M. Ferrero, Jr., and B. Trenor. 2002. Mechanistic investigation of extracellular K^+ accumulation during acute myocardial ischemia: a simulation study. *Am. J. Physiol. Heart Circ. Physiol.* 283:H490–H500.
36. Livshitz, L. M., and Y. Rudy. 2007. Regulation of Ca^{2+} and electrical alternans in cardiac myocytes: role of CaMKII and repolarizing currents. *Am. J. Physiol. Heart Circ. Physiol.* 292:H2854–H2866.
37. Pieske, B., L. S. Maier, V. Piacentino III, J. Weisser, G. Hasenfuss, and S. Houser. 2002. Rate dependence of $[Na^+]i$ and contractility in nonfailing and failing human myocardium. *Circulation.* 106:447–453.
38. Despa, S., M. A. Islam, C. R. Weber, S. M. Pogwizd, and D. M. Bers. 2002. Intracellular Na^+ concentration is elevated in heart failure but Na/K pump function is unchanged. *Circulation.* 105:2543–2548.
39. Shannon, T. R., F. Wang, and D. M. Bers. 2005. Regulation of cardiac sarcoplasmic reticulum Ca release by luminal [Ca] and altered gating assessed with a mathematical model. *Biophys. J.* 89:4096–4110.
40. McIntosh, M. A., S. M. Cobbe, and G. L. Smith. 2000. Heterogeneous changes in action potential and intracellular Ca^{2+} in left ventricular myocyte sub-types from rabbits with heart failure. *Cardiovasc. Res.* 45:397–409.
41. Antzelevitch, C., and J. Fish. 2001. Electrical heterogeneity within the ventricular wall. *Basic Res. Cardiol.* 96:517–527.
42. Gaita, F., C. Giustetto, F. Bianchi, C. Wolpert, R. Schimpf, R. Riccardi, S. Grossi, E. Richiardi, and M. Borggrefe. 2003. Short QT syndrome: a familial cause of sudden death. *Circulation.* 108: 965–970.
43. Antzelevitch, C. 2005. Cardiac repolarization. The long and short of it. *Europace.* 7(s2):S3–S9.
44. Zhang, T., and J. H. Brown. 2004. Role of Ca^{2+}/calmodulin-dependent protein kinase II in cardiac hypertrophy and heart failure. *Cardiovasc. Res.* 63:476–486.
45. Hund, T. J., and Y. Rudy. 2004. Rate dependence and regulation of action potential and calcium transient in a canine cardiac ventricular cell model. *Circulation.* 110:3168–3174.
46. Saucerman, J. J., and D. M. Bers. 2007. CaM mediates differential sensitivity of CaM kinase and calcineurin to local Ca^{2+}. *Biophys. J.* 92:365a. (Abstr.)
47. Weber, C. R., V. Piacentino III, K. S. Ginsburg, S. R. Houser, and D. M. Bers. 2002. Na^+-Ca^{2+} exchange current and submembrane $[Ca^{2+}]$ during the cardiac action potential. *Circ. Res.* 90:182–189.